Taylor & Francis
Taylor & Francis Group

Journal of Intelligent Transportation Systems
Technology, Planning, and Operations

ISSN: 1547-2450 (Print) 1547-2442 (Online) Journal homepage: http://www.tandfonline.com/loi/gits20

# Real-time queue length estimation using event-based advance detector data

Chengchuan An, Yao-Jan Wu, Jingxin Xia & Wei Huang

**To cite this article:** Chengchuan An, Yao-Jan Wu, Jingxin Xia & Wei Huang (2018) Real-time queue length estimation using event-based advance detector data, Journal of Intelligent Transportation Systems, 22:4, 277-290, DOI: 10.1080/15472450.2017.1299011

**To link to this article:** https://doi.org/10.1080/15472450.2017.1299011

Accepted author version posted online: 27 Mar 2017.
Published online: 03 Apr 2017.

JOURNAL OF INTELLIGENT TRANSPORTATION SYSTEMS, 2018
VOL. 22, NO. 4, 277–290
http://dx.doi.org/10.1080/15472450.2017.1299011

Taylor & Francis
Taylor & Francis Group

# Real-time queue length estimation using event-based advance detector data

Chengchuan An[a], Yao-Jan Wu[b], Jingxin Xia[a], and Wei Huang[a]

[a]Intelligent Transportation System Research Center, Southeast University, Nanjing, P.R. China; [b]Department of Civil Engineering and Engineering Mechanics, University of Arizona, Tucson, AZ, USA

**ABSTRACT**

Real-time queue length information at signalized intersections is useful for both performance evaluation and signal optimization. Previous studies have successfully examined the use of high-resolution event-based data to estimate real-time queue lengths. Based on the identification of critical breakpoints, real-time queue lengths can be estimated by applying the commonly used shockwave model. Although breakpoints can be accurately identified using lane-by-lane detection, few studies have investigated queue length estimation using single-channel detection, which is a common detection scheme for actuated signal control. In this study, a breakpoint misidentification checking process and two input-output models (upstream-based and local-based) are proposed to address the overestimation and short queue length estimation problems of breakpoint-based models. These procedures are integrated with a typical breakpoint-based model framework and queue-over-detector identification process. The proposed framework was evaluated using field-collected event-based data along Speedway Boulevard in Tucson, Arizona. Significant improvements in maximum queue length estimates were achieved using the proposed method compared to the breakpoint-based model, with mean absolute errors of 35.7and 105.6ft., respectively.

**ARTICLE HISTORY**
Received 7 March 2016
Revised 8 September 2016
Accepted 5 February 2017

**KEYWORDS**
High-resolution event-based data; input-output model; real-time queue length estimation; shock wave model

## Introduction

Queue length is one of the most important performance measures for signalized intersections because it is easy to interpret and highly correlated to other performance measures, including delay (Sharma, Bullock, & Bonneson, 2007; Ban, Hao, & Sun, 2011), number of stops (Stephanopoulos, Michalopoulos, & Stephanopoulos, 1979), and travel time (Liu & Ma, 2009). Queue length data help traffic engineers better evaluate the performance of traffic systems and make well-grounded decisions for improvements. For signal timing optimization, especially under congested conditions, effective signal control strategies to relieve oversaturation could be developed based on queue lengths (Lieberman, Chang, & Prassas, 2000; Lieberman & Chang, 2005; Hu, Wu, & Liu, 2013).

Most existing queue length estimation methods are based on two fundamental models: the input-output model (Webster, 1958; Newell, 1960; Robertson, 1969; Strong & Rouphail, 2006) and the shockwave model (Lighthill & Whitham, 1955; Richards, 1956; Stephanopoulos et al., 1979; Michalopoulos, Stephanopoulos, & Pisharody, 1980). These models were utilized to estimate either average queue length over a relatively long time interval (e.g., 15 min or 1 hour) or real-time maximum queue length for individual cycles. The average queue length estimation methods, including the Highway Capacity Manual (2010) method, typically use aggregated traffic flow data (e.g., traffic volume every 15 min) to represent a steady traffic state. These models are appropriate for planning-level analysis but are not adequate for real-time queuing analysis. With the growing need for real-time traffic management (Wu, An, Ma, & Wang, 2011), including traveler information services and adaptive signal control, real-time queue estimation has recently gained much attention.

A number of models have been proposed for real-time queue length estimation using various data sources, including volume and occupancy collected by point detectors (Mück, 2002; Geroliminis & Skabardonis, 2006; Sharma et al., 2007; Skabardonis & Geroliminis, 2008; Chang, Talas, & Muthuswamy, 2013), GPS vehicle trajectories (Cheng, Qin, Jin, Ran, & Anderson, 2011; Cheng, Qin, Jin, & Ran, 2012), probe vehicles (Comert & Cetin, 2009; Claudel, Hofleitner, Mignerey, & Bayen, 2009), travel time (Ban et al., 2011; Hao, Ban, Guo, & Ji, 2014; Hao, Ban, & Whon Yu, 2015), mobile data (Hao & Ban, 2015), and video images (Zheng, Ma, Wu, & Wang, 2013). Going even further, some models incorporated

**CONTACT** Jingxin Xia xiajingxin@seu.edu.cn Intelligent Transportation System Research Center, Southeast University, No. 35 Jinxianghe Road, Nanjing 210096, P.R. China.
Color versions of one or more of the figures in the article can be found online at www.tandfonline.com/gits.

traffic platoon dispersion effects (Robertson & Bretherton, 1991; Mück, 2009), actuated signal timing (Viti & van Zuylen, 2009), and more advanced statistical techniques, such as Markov chains (Viti & van Zuylen, 2004; Geroliminis & Skabardonis, 2005) and Kalman filters (Lee, Wong, & Li, 2015; Anusha, Sharma, Vanajakshi, Subramanian, & Rilett, 2016), to achieve more realistic and robust modeling performance. These studies have demonstrated applications of fine-grained data to estimate real-time queue lengths. One of the most promising data sources is high-resolution signal event-based data (referred to as "event-based data" for the rest of the paper), including signal phase change events and vehicle-detector actuation events at a resolution of every second or better. These data are becoming more accessible as an increasing number of signal controllers and central traffic management systems collect and archive these data in real time. Liu, Wu, Ma, & Hu (2009) proposed a breakpoint-based queue length estimation method for situations where queues grow beyond the advance detectors, known as queue-over-detector (QOD). The critical step in their method was to identify the breakpoints indicating the changes in traffic states during queue formation and discharge at the detector location. Then, the maximum queue length was estimated by reconstructing shockwave profiles based on shockwave theory. According to a test by Liu et al., lane-by-lane detection resulted in better queue length estimates compared to single-channel detection. However, further tests are needed to explore queue length estimation with single-channel detection. Single-channel detection is widely used for actuated signal control in the field.

There are two major problems when applying the breakpoint-based model to estimate queue lengths with single-channel detection. The first is the misidentification of breakpoints. Breakpoints are identified based on sudden changes in time gaps between consecutive actuations. However, gaps reported by single-channel detectors represent the headways of vehicles in multiple lanes. The times when the critical gaps appear in individual lanes may be misidentified with significant delay. This is similar to the issue of single-channel detection having difficulty in gapping out a phase on multi-lane approaches (Tian & Urbanik, 2006). As a consequence, queue length will be overestimated. The second problem is that volume is not measured directly by single-channel detectors. Thus, the input-output model cannot be used in situations where the breakpoint-based model is inadequate, including short queue lengths (queues that do not reach the detector) and long queue lengths (queues that stretch beyond the detector) when breakpoints are misidentified.

This paper proposes a method of estimating real-time maximum queue lengths for individual cycles using event-based data, specifically with single-channel advance detection (approximately 150–400 feet upstream of the stop bar). To address the limitations of the breakpoint-based model, a misidentification checking process was created to determine when the breakpoint-based model can be applied to individual cycles with a low likelihood of breakpoint misidentification. For situations when the breakpoint-based model is not suitable, two input-output models (one upstream-based and one local-based) were developed based on a simple flow rate estimation model using vehicle actuation data from advance detectors at local and upstream intersections as inputs. The local-based model was used to estimate short queue lengths, while the upstream-based model was used to estimate long queue lengths. The proposed method is compatible with various standard detectors, including inductive loop detectors and video-based detectors.

## Methodology

### Framework

The problem this study addressed is defined as follows: given event-based data collected from single-channel advance detectors at local intersection $i$ and upstream intersection $i + 1$ up to current time $t$, estimate the maximum queue length in the associated movement for the immediately preceding cycle at intersection $i$. This methodology focuses on maximum queue lengths for through lanes.

Figure 1 illustrates the framework of the proposed method. At time $t$, intersections $i$ and $i + 1$ are running the $kth$ and $k'th$ cycle, respectively. The queue estimation process runs until both cycles end. First, QOD identification and breakpoint identification are conducted at each of the intersections for both the $kth$ and $k'th$ cycles to classify the queue that develops as either a long queue or a short queue. Then, if QOD occurs at intersection $i$, a misidentification checking process determines whether to use the breakpoint-based model or the upstream-based input-output model to estimate the long length. If QOD does not occur, a local-based input-output model is used to estimate the short queue length. Note that the input-output models also incorporate a flow rate estimation model. Essentially, the proposed framework is a maximum queue length estimation strategy designed to overcome the limitations of the breakpoint-based model with single-channel detection.

### Queue-over-detector and breakpoint identification

Figure 2 shows four stages of queue formation and discharge during a typical signal cycle with QOD. Each stage is identified by distinct detector and signal states. In

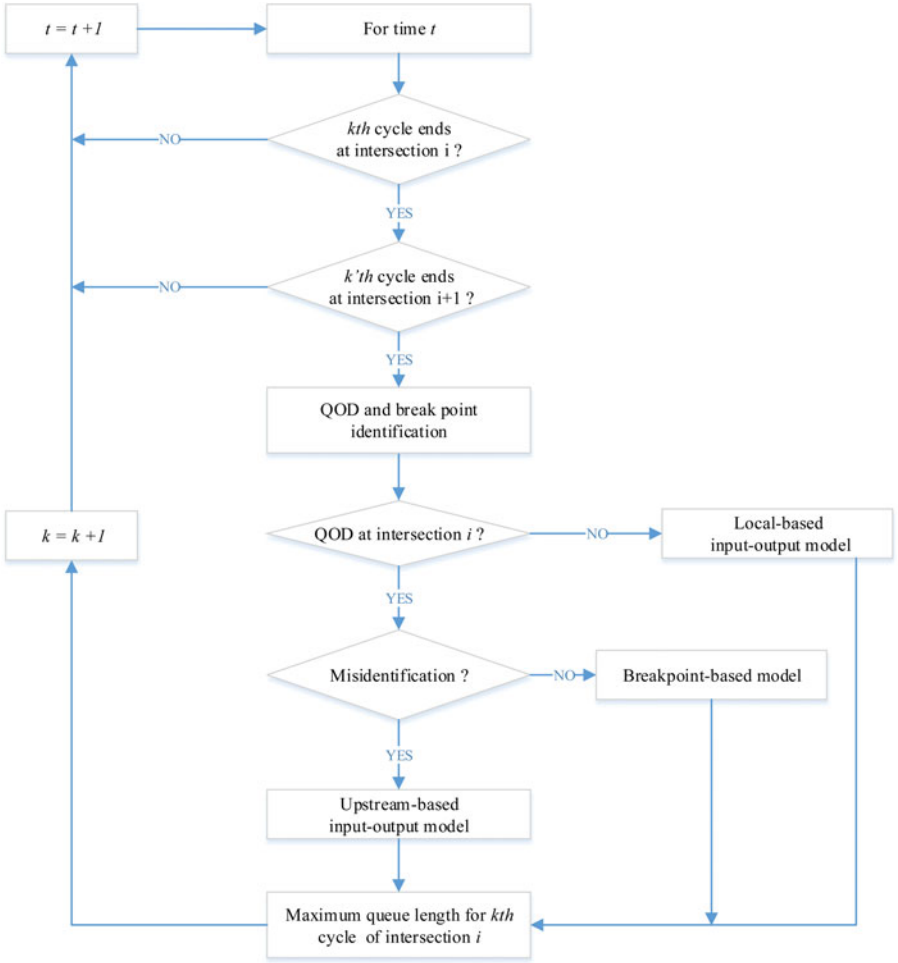


**Figure 1.** Framework of proposed method.

Figure 2, the dark blue bars represent vehicle actuations, and the blank spaces between consecutive vehicle actuations represent the gaps between vehicles.

- **Stage 1** begins at the start of effective red and ends when the downstream queue reaches the detector (point A). During this stage, arriving vehicles stop due to the red light, but the queue length is still shorter than the distance from the stop bar to the detector.
- **Stage 2** is between point A and point B. Point B is the time after the start of the green phase when the queue discharge wave reaches the detector. During

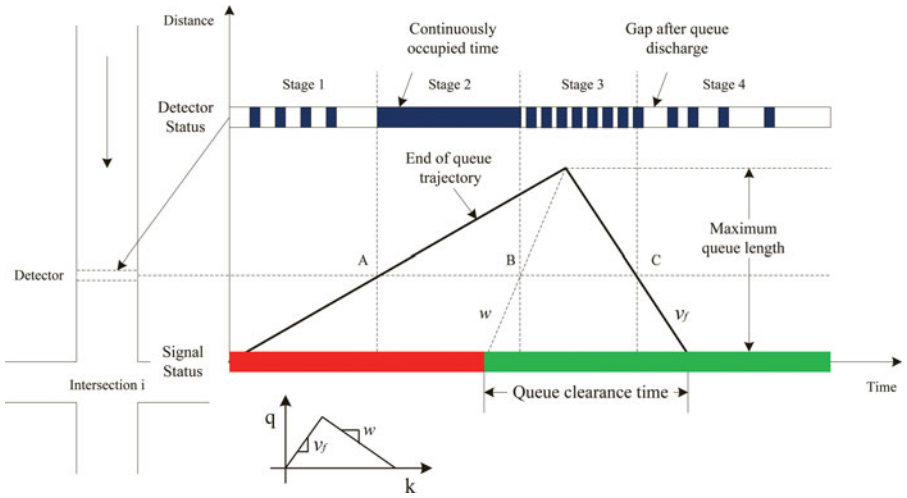


**Figure 2.** Four typical stages during cycles with QOD.

stage 2, the detector is continuously occupied by stopped vehicles.

- **Stage 3** is between point B and point C. Point C is the time when the upstream end of the queue passes the detector. During stage 3, queued vehicles start to discharge, and the maximum queue length occurs when the last vehicle in the queue begins to move. The gaps between consecutive vehicle actuations are approximately equal to the saturation headway.
- S**tage 4** is between point C and the end of the effective green. During this stage, the queue has discharged at the detector and arriving flow can pass through intersection without impedance. The gaps are larger compared to stage 3.

The points A, B, and C were defined as breakpoints by Liu et al. (2009). With a well-defined q-k fundamental diagram, the maximum queue length could be determined using any two of these three points, although points B and C are used in most studies (Liu et al., 2009). In our study, the q-k relationship is assumed to be triangular (see the bottom of Figure 2). Thus, the speeds of the shockwaves that pass points B and C are constant and equal to the queue discharge wave speed and free flow speed corresponding to the slopes of the right and left branches of the q-k fundamental diagram, respectively.

Since the speed of the queue discharge wave (passing through point B) is constant, such that point B occurs at a consistent time after the start of effective green, QOD could be identified when the duration of the continuously occupied status before point B exceeds a certain threshold ($th_1$), and point C could be identified when gap time after point B exceeds a certain threshold ($th_2$). This threshold-based approach is accurate enough to determine whether or not QOD occurs Liu et al. (2009). However, significant misidentification problems of point C may arise when single-channel detection is used. These problems are discussed further in the next section.

### *Misidentification checking*

Figure 3(a) illustrates a typical QOD scenario on a one-way two-lane approach where misidentification of point C occurs with single-channel detection. Assume the maximum queue length on this approach is in Lane 2. The signal statuses are shown for the phases associated with through movements at intersection $i$ and $i+1$. The red and blue lines are vehicle trajectories in Lane 1 and Lane 2, respectively. The red trajectories are shown only after queue discharge in Lane 2. $t_{g,i}^k$ and $t_{r,i}^k$ represent the start times of the effective red and green of the $kth$ cycle at intersection $i$, respectively. In this case, the single-channel detector fails to capture the headway increase in Lane 2 (see actual gap in Lane 2) because arriving vehicles in Lane 1 are also detected (note the gap identified by the detector). As a consequence, although the end of the queue has passed the detector in Lane 2 (see actual point C), the critical gap cannot be identified until both lanes together have no vehicle detections for at least $th_2$ (see identified point C).

Arriving traffic, especially traffic arriving after queue discharge, could significantly impact the accurate identification of point C under single-channel detection. Thus, a real-time progression band was created to represent traffic that departed from the upstream intersection. In this study, the progression band was associated with the upstream green for the through movement (see the shaded area in Figure 3(a)), with the underlying assumption that upstream through traffic comprises the majority of arriving traffic at the downstream intersection. This is approximately true on a typical urban arterial. However, it is also possible to add more progression bands as long as other movements (e.g., left- and right-turn movements at the upstream intersection) are also comparably significant.

In the QOD scenario, the actual queue length is a possible value between the minimum and maximum possible queue lengths corresponding to the distance from stop bar to the detector and the queue length associated with identified point C, respectively (see Figure 3(a)). If point C is not misidentified, the actual queue length is equal to the maximum possible queue length. In this study, the likelihood of misidentification was determined by the relative positions between the real-time progression bands and the identified point C. Some critical times were defined and used to determine the relative positions. The arrival times of the leading and lagging boundaries of the progression band are calculated as $t_{r,i+1}^{k+1'} + TT$ and $t_{g,i+1}^{k'} + TT$, respectively, where $TT$ is the free flow travel time from upstream intersection $i+1$ to local intersection $i$. $t_{qc,i}^k$ and $t_{d,i}^k$ present the times when the maximum and minimum possible queues are cleared at local intersection $i$, which can be calculated using Equations (1) and (2), respectively.

$$t_{qc,i}^k = t_{c,i}^k + tt \tag{1}$$

Where $t_{c,i}^k$ is the time when point C is identified and $tt$ is the free flow travel time from the detector to the stop bar.

$$t_{d,i}^k = t_{r,i}^k + d\left(\frac{1}{w} + \frac{1}{v_f}\right) \tag{2}$$

Where $d$ is the distance from the stop bar to the detector; $v_f$ and $w$ are the free flow speed and queue discharge wave speed, respectively. Note that Equations (1) and (2) are all based on the assumption of a triangular q-k fundamental diagram.

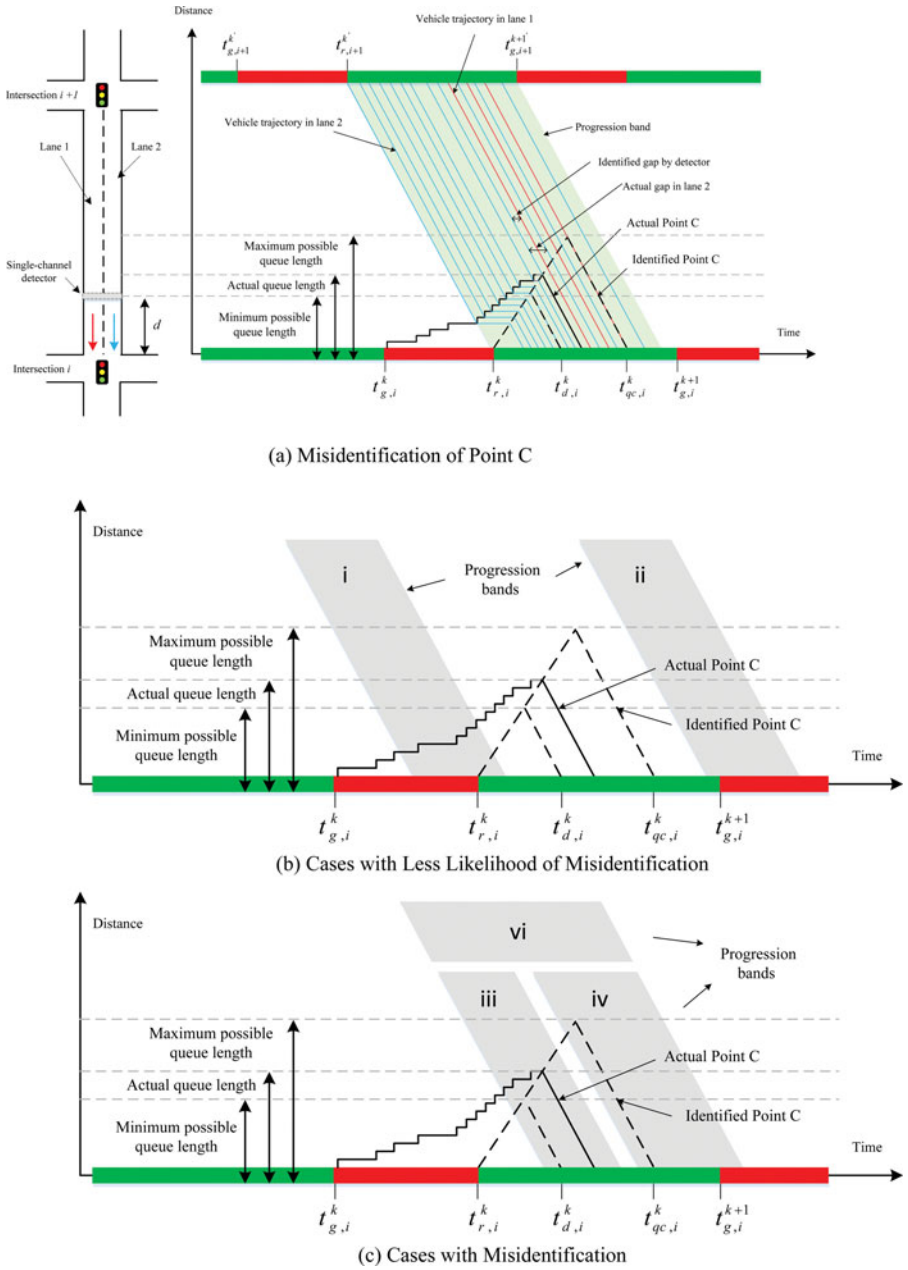


**Figure 3.** Impact of arriving traffic on point c identification.

Figure 3 (b) illustrates situations where the progression bands arrive before $t_{d,i}^{k}$ or after $t_{qc,i}^{k}$, shown as progression bands i and ii in Figure 3 (b), respectively. In these situations, traffic is fully stopped or arrives after the queue discharge, and misidentification of point C is less likely. Hence, the breakpoint-based model is adequate in these situations. In other situations, point C may easily be misidentified with the interference of arrival traffic (see situations illustrated in Figure 3(c)). Note that the progression band iii in Figure 3 (c) may not create a misidentification scenario as the traffic may have to fully stop, similar to the situation with progression band i in Figure 3 (b); or may present a typical misidentification scenario when the traffic is not fully stopped and the tail of the arrival traffic causes the misidentification. In this study, this ambiguous situation was considered as a misidentification case. The misidentification situations were addressed with a more reliable input-output model, which is described in the following section.

### *Breakpoint-based model*

If the misidentification of point C is unlikely (the misidentification process in the framework shows NO), maximum queue length $Q_i^k$ during the *kth* cycle at intersection *i* can be calculated using a breakpoint-based model, such as the one shown in Equation (3).

$$Q_i^k = \frac{v_f\left(t_{c,i}^k - t_{r,i}^k\right) + d}{v_f/w + 1} \tag{3}$$

Equation (3) is a simplified version of the model proposed by Liu et al. (2009) with vehicle acceleration ignored and vehicles are assumed to have a constant free flow speed when discharging. Although this simplification may cause queue length overestimation to some extent, such error could be reduced by implementing the original model (Liu et al., 2009) with additional modeling of the vehicle acceleration process. In this study, for simplicity, Equation (3) is used.

### Input-output models

As illustrated above, with single-channel detection, the breakpoint-based model is not capable of accurately estimating queue length when short queues form or point C is misidentified. The solution to this problem is to use the input-output model (Liu et al., 2009). The input-output model requires the flow rate of both arriving and departing traffic. Typically, arriving traffic can be measured by advance detectors. Departing traffic can be measured either by stop bar detectors or by assuming a departure profile based upon the actual green times (Day et al., 2014). Recall that volume is not measured directly by single-channel detectors. The number of vehicle actuations is normally less than actual traffic counts. Thus, a conversion from vehicle actuation information to traffic counts or flow rate is necessary. Typically, a probability-based model would be developed to estimate flow rate based on vehicle actuations (Wu, Zhang, & Wang, 2010). However, probability-based models are more statistically suitable for estimating volume over a relatively long aggregation interval (e.g., one hour) rather than individual cycles. In our study, an input flow rate estimation model was developed using vehicle actuation data at two advance locations: a local advance detector and the stop bar of the upstream intersection. Then, an incremental algorithm was developed using the estimated flow rate as an input for maximum queue length estimation. The input flow rate and maximum queue length estimation models are two input-output models distinguished by the location of input flow rate (the local-based and upstream-based input-output models as mentioned in framework). Parameter calibration is discussed at the end of this section.

### Input flow rate estimation

Figure 4 illustrates the locations where traffic flow can be used as an input for the westbound through lane group at intersection *i*. Assuming no spillback will block intersection *i* and $i + 1$, the discharge flow at the stop bars of upstream intersection $i + 1$ can be used as the input flow to intersection *i*, while arriving flow at the local advance detector (detector *i*) is only detected when the queue has not reached the detector location. Thus, the input flow rate estimation problem in this study includes two cases: (1) arrival flow rate estimation using vehicle actuation data from the local advanced detector (detector *i*) when QOD does not occur and (2) discharge flow rate estimation using vehicle actuation data from the advance detector (detector $i + 1$) at the upstream intersection when QOD does occur.

**Case 1. Arrival flow rate estimation at local advance detector without queue-over-detector**

Since only a short queue developed, traffic arriving at the local advance detector can be approximately considered as unimpeded flow. A generalized parameter $\bar{h}$ is defined to represent the average headway for unimpeded flow within each vehicle actuation. Because $\bar{h}$ is a time- and site-dependent variable, it is assumed to be identical for a certain time period (e.g., 1 hour) with similar traffic conditions at a particular site. Thus, the conversion from the duration of each vehicle actuation to flow rate in discrete time intervals can be accomplished using Equation (4) and (5).

$$N = max\left(1,\ T_a/\bar{h}\right) \tag{4}$$

$$q\,(t) = N/T_a \quad for\ t = 1, 2, 3, \ldots, \frac{T_a}{\Delta_t} \tag{5}$$

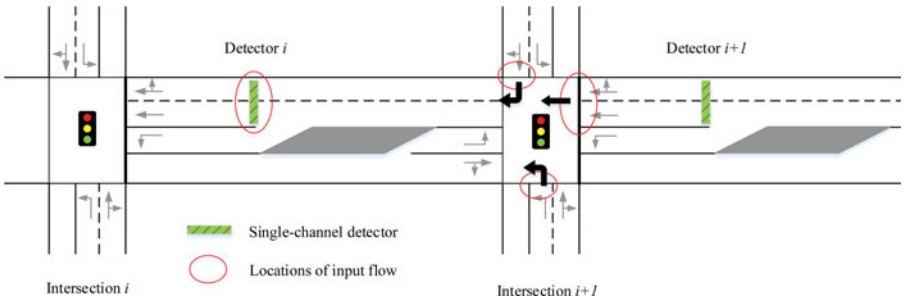


**Figure 4.** Advance locations for input flow rate estimation.

Where $N$ is the total number of arriving vehicles, $\bar{h}$ is the parameter needing to be calibrated, $q(t)$ is the flow rate of the $tth$ interval within $[t_{on}, t_{off}]$, $t_{on}$ and $t_{off}$ are the times when vehicle actuation is on and off, and $t_{off} - t_{on} = T_a$, $\Delta_t$ is the discrete time interval (e.g., 1s), and $\lfloor\rfloor$ is the floor operator. The max operator in Equation (4) ensures that at least one vehicle is counted for each vehicle actuation. The gaps between actuations will generate zero flow rate.

**Case 2. Discharge flow rate estimation at the stop bar of the upstream intersection**

In Case 2, only the discharge flow of the through movement is estimated, and other minor movements (e.g., left and right turns) are assumed to be known and uniformly distributed within the red time of the through movement phase. To better characterize the flow discharging process, two scenarios are investigated and modeled independently, as illustrated in Figure 5.

*Scenario 1: QOD does* not *occur at the upstream intersection (shown in Figure 5(a)).*

In this scenario, arriving traffic is also considered as unimpeded flow. The same assumption and parameter definition are used as in Case 1. Specifically, vehicles arriving during time $[t^{k'}_{g,i+1} - tt, t^{k'}_{d,i+1} - tt]$ at the advance detector are assumed to discharge during green time $[t^{k'}_{r,i+1}, t^{k'}_{d,i+1}]$. $t^{k'}_{d,i+1}$ is the time when the end of the maximum possible queue (with length of $d$) of the $k'th$ cycle passes through intersection $i + 1$ and can be calculated using Equation (2). Then, the discharging flow rate for each discrete interval $\Delta_t$ within $[t^{k'}_{r,i+1}, t^{k'}_{d,i+1}]$ can be calculated using Equations (6) and (7).

$$N = \sum_{i=1}^{n} max\left(1,\ T_{a,i}/\bar{h}\right) \tag{6}$$

$$q(t) = \frac{N}{\left(t^{k'}_{d,i+1} - t^{k'}_{r,i+1}\right)} \ for\ t = 1, 2, 3, \ldots, \frac{t^{k'}_{d,i+1} - t^{k'}_{r,i+1}}{\Delta_t} \tag{7}$$

Where $n$ is the total number of actuations during $[t^{k'}_{g,i+1} - tt, t^{k'}_{d,i+1} - tt]$, $T_{a,i}$ is the duration of the $ith$ actuation, $\bar{h}$ is the parameter to be calibrated, $q(t)$ is the discharge flow rate of the $tth$ interval within $[t^{k'}_{r,i+1}, t^{k'}_{d,i+1}]$. For the time interval $[t^{k'}_{d,i+1}, t^{k'+1}_{g,i+1}]$, the discharge flow rate can be calculated by each actuation within $[t^{k'}_{d,i+1} - tt, t^{k'+1}_{g,i+1} - tt]$ using Equations (4) and (5).

*Scenario 2 : QOD occurs at the upstream intersection (shown in Figure 5(b)).*

In this scenario, the discharge flow rate during time $[t^{k'}_{r,i+1}, t^{k'}_{qc,i+1}]$ may not remain at the saturation flow rate because of potential misidentification. Hence, another generalized parameter $\bar{h}_s$ is introduced to represent this relatively intensive discharge flow rate during $[t^{k'}_{r,i+1}, t^{k'}_{qc,i+1}]$. $\bar{h}_s$ is also assumed to be constant for a certain time period at a particular site. The discharge flow rate can be calculated using Equation (8).

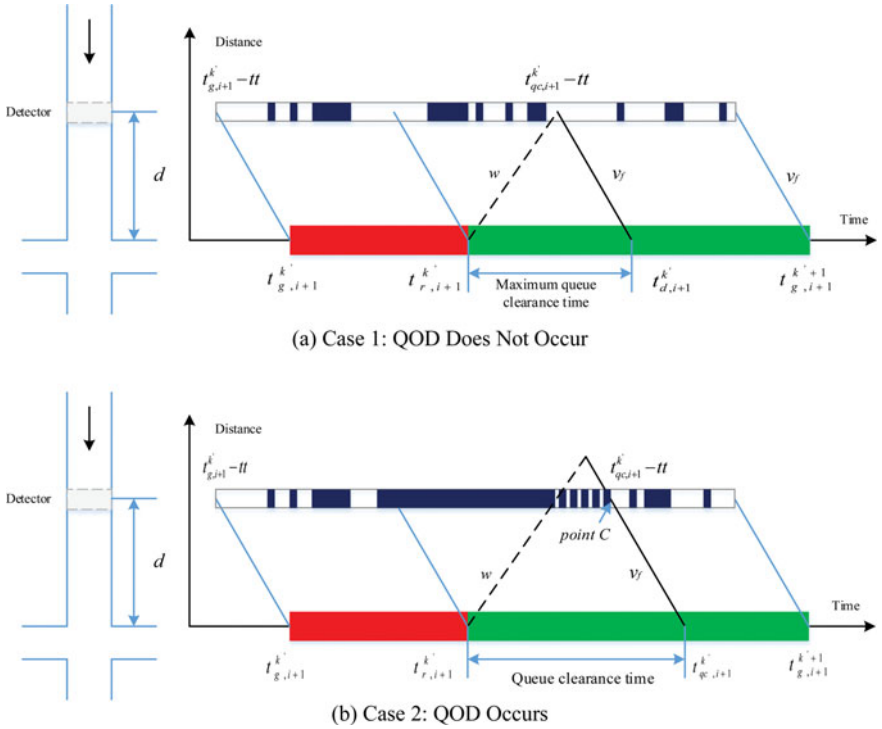


**Figure 5.** Discharging flow rate estimation for upstream intersection.

$$q(t) = \frac{1}{\bar{h}_s} \text{ for } t = 1, 2, 3, \ldots, \frac{t^{k'}_{qc,i+1} - t^{k'}_{r,i+1}}{\Delta_t} \quad (8)$$

Where $\bar{h}_s$ is the parameter to be calibrated and $q(t)$ is the discharge flow rate for the $tth$ interval within $[t^{k'}_{r,i+1}, t^{k'}_{qc,i+1}]$. The discharge flow rate during $[t^{k'}_{qc,i+1}, t^{k'+1}_{g,i+1}]$ can be calculated using the same procedure as Scenario 1. In situations when point C is detected late in the next cycle, the entire green time of the $k'th$ cycle will have a uniform discharge flow rate calculated by Equation (8).

For the estimated input flow rates (either estimated at the local or the upstream intersection), a series of discrete intervals with different discharging flow rates can be generated for each cycle. At the local advance detector, only the series for the current cycle is needed. At the stop bar of the upstream intersection, several of the most recent cycles (e.g., the previous three to five cycles) should be combined together. The exact number of cycles is highly dependent on the free flow travel time between the upstream and downstream intersections.

### *Maximum queue length estimation*

Figure 6 illustrates a maximum queue length estimation scenario using discharge flow rate at the stop bar of the upstream intersection. Generally, there are three stages (stages I-III in Figure 6) of vehicle progression. Vehicles that depart from the upstream intersection during $[t^k_{g,i} - TT, t^k_{r,i} - TT]$ (stage I) must stop at the downstream intersection due to the red light. The queue length $Q_I$ at the end of stage I can be calculated by Equation (9).

$$Q_I = \sum_t q(t)\,\Delta_t \beta h_j \text{ for } t = 1, 2, 3, \ldots, \frac{t^k_{r,i} - t^k_{g,i}}{\Delta_t} \quad (9)$$

Where $q(t)$ is the flow rate of $tth$ interval during $[t^k_{g,i} - TT, t^k_{r,i} - TT]$, $h_j$ is the jam space headway, and $\beta$ is the lane utilization ratio representing the queue length distribution across multiple lanes.

Stages II and III represent vehicles that depart during time $[t^k_{r,i} - TT, t^{k+1}_{g,i} - TT]$, which may or may not join the end of the queue at intersection $i$, depending on whether or not the queue has cleared. During stage II, vehicles join the queue, and in state III, they do not. To describe the dynamic queue accumulation process, an incremental algorithm is proposed. The algorithm will calculate accumulated queue length by moving forward at a time interval $\Delta_t$ incrementally until the queue discharge wave reaches the end of the queue, when the last vehicle in the queue begins to move and no vehicles remained stopped. The algorithm is summarized below.

**Step 1:** increments = 1, queue length $QL = Q_I$

**Step 2:** total increment time $TIT$ = increments* $\Delta_t$

**Step 3:** if $TIT < QL(\frac{1}{w} + \frac{1}{v_f})$, increments ++, $QL = QL + q(t)\,\Delta_t \beta h_j$, return to step 2; if not, move to next step. Here, $t$ presents the $tth$ interval after time $t^k_{r,i} - TT$.

**Step 4:** Maximum queue length = $QL$

This algorithm can also use the arrival flow rate at the local advance detector as an input. The only difference in the algorithm is to substitute $TT$ with $tt$ (the free flow travel time from the detector to the stop bar). Note that the estimated maximum queue length may exceed the implied constraint (maximum queue length is shorter than the distance from the detector to the stop bar). Thus, the maximum queue length should be constrained by $max(QL, d)$.

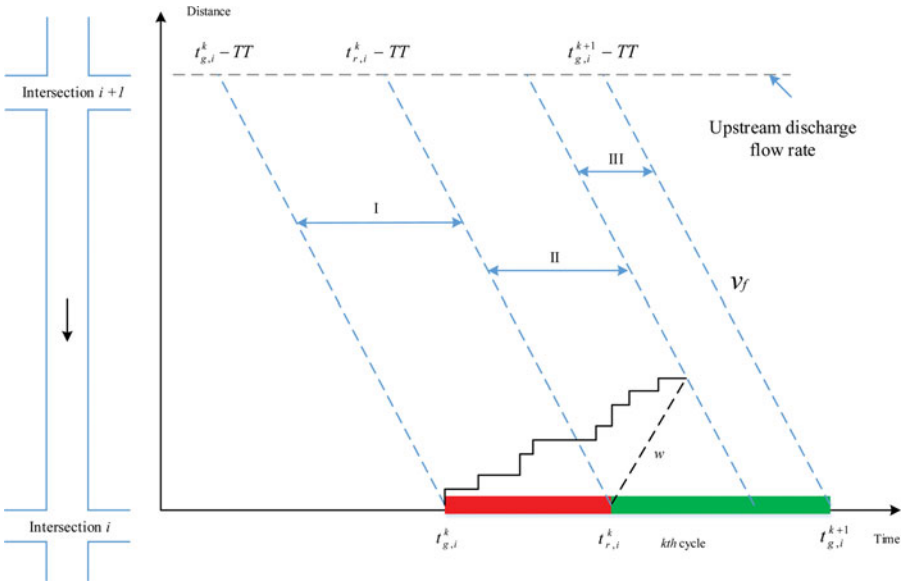


**Figure 6.** Maximum queue length estimation based on upstream discharge flow rate.

Two input-output models are defined based on the input flow rate estimation model and the maximum queue length estimation model described above. The local-based model uses arrival flow rate at the local advance detector (Case 1) as inputs and is only able to estimate short queue lengths. The upstream-based model uses discharge flow rate at the stop bar of upstream intersection (Case 2) as inputs and can estimate both short and long queue lengths.

### *Parameter calibration*

The local-based model has one parameter ($\bar{h}$) that must be calibrated, while the upstream-based model has two parameters ($\bar{h}$ and $\bar{h}_s$) that must be calibrated. Other parameters, such as queue discharge wave speed, free flow speed, jam space headway, and lane utilization ratio, are assumed to be known already. $h$ and $\bar{h}_s$ can be calibrated using either of two potential approaches. One approach is based on field-collected traffic flow rates at corresponding locations. Another is based on ground truth maximum queue length collected at the local intersection. The former approach requires collection of both discharge and arrival flow rates at the upstream and local intersections, respectively. Further, calibration of the turning ratio at the downstream intersection may be necessary. The latter approach was adopted in this study given its lower data collection requirements and calibration effort. For a time period with similar traffic conditions and $n$ cycles, the objective function is to minimize the mean square error (MSE) as illustrated in Equation (10).

$$\text{Min} \ \frac{\sum_{i=1}^{n} (Q_i - \hat{Q}_i)^2}{n} \tag{10}$$

Where $Q_i$ and $\hat{Q}_i$ are the ground truth maximum queue length and estimated maximum queue length, respectively, of the *ith* cycle. Consider that the parameters have a relative narrow solution space according to their implied definitions. In this study, the solution space was chosen as [1.0, 5.0]. Every potential combination within this solution space was evaluated. Notice that the local-based model is only able to estimate the short queue lengths. Thus, only data from cycles without QOD were used for parameter calibration.

## Implementation

### *Test sites*

Two intersections on Speedway Boulevard in Tucson, Arizona, were selected as test sites for the proposed method. The location and detector configurations of these intersections are shown in Figure 7. Maximum queue length estimation for the westbound through movement

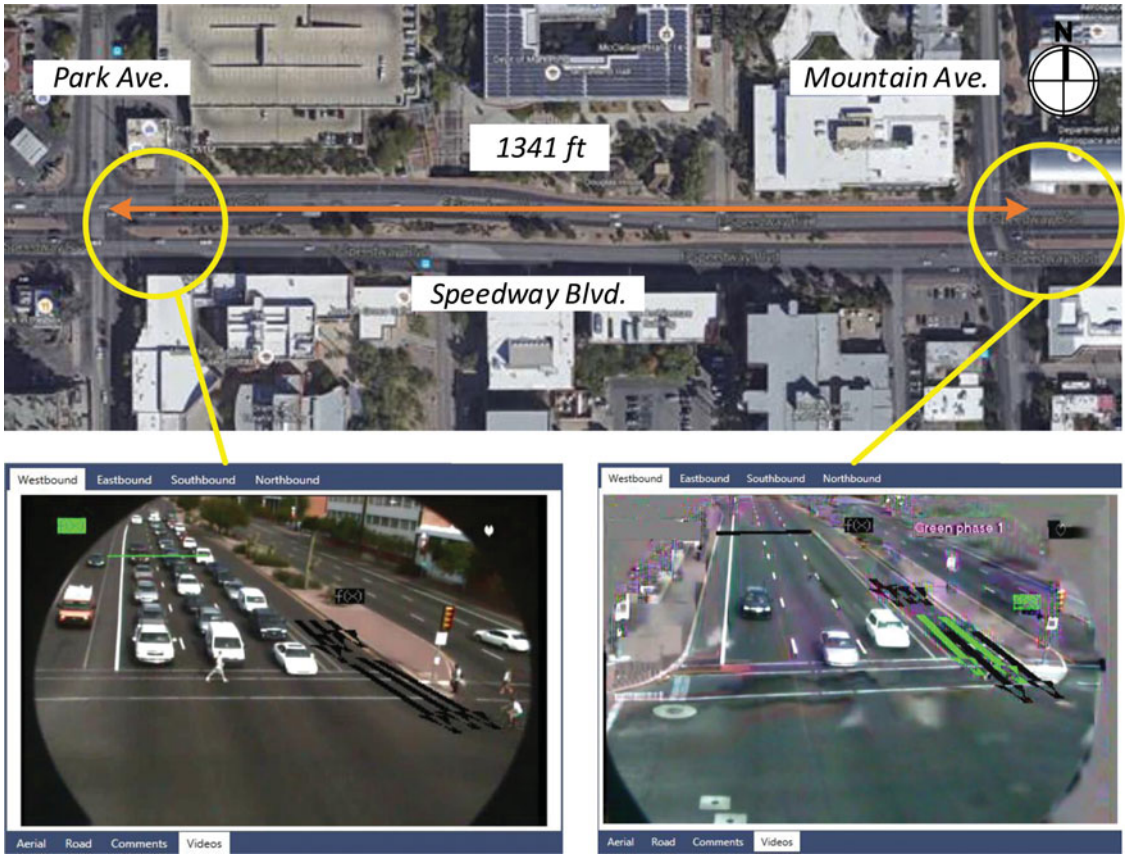


**Figure 7.** Location and detector configurations of the selected intersections.

**Table 1.** Model parameters.

| Label | Parameter | Speedway & Park | Speedway & Mountain |
|---|---|---|---|
| $w$ | Queue discharge wave speed | 18 mi/h | 18 mi/h |
| $v_f$ | Free flow speed | 35 mi/h | 35 mi/h |
| $h_j$ | Jam space headway | 25 ft | — |
| $\beta$ | Lane utilization ratio | 0.45 | — |
| $th_1$ | QOD identification threshold | 12 s | 12 s |
| $th_2$. | Point C identification threshold | 2 s | 2 s |

at Speedway and Park Avenue was of special interest. The intersections used a video-based detection system to trigger and send real-time vehicle actuations to the signal controller. The virtual detection bars were configured as single-channel detectors. Although reconfiguring single-channel detection to lane-by-lane detection for video-based detectors is relatively easy, the purpose of this study was to show the performance of the proposed model with only single-channel detection, irrespective of specific detection technologies. The space between the virtual detectors and the stop bars along Speedway at its intersections with Park and Mountain Avenue were large enough to store 6.5 and 6 passenger cars, respectively. These capacities translate to a length of approximately 160 ft. (49 m) and 148 ft. (45 m) given a jam space headway of 25 ft. (7.5 m). The speed limit along Speedway was 35 mph (56 km/h) and was assumed to represent the free flow speed.

There were two primary reasons for choosing these two intersections as test sites. First, the intersections were relatively congested throughout the day. Second, the Speedway and Mountain intersection was operating under fully actuated control mode, while the Speedway and Park intersection was under signal coordination during the day. This difference in signal operation meant that various traffic arrival patterns could be expected for the westbound through movement at Speedway and Park.

## Data collection

The data used in this study were collected from MaxView$^{TM}$, a central traffic management system. MaxView collected and archived video image data and real-time event-based data with a resolution of one second. Trained technicians manually determined the ground truth maximum queue length for every cycle based on video observation. In this study, data from four typical weekdays were used (Tuesday, July 14–Thursday, July 16, 2015 and Wednesday, July 22, 2015). Data collected during July 14–16 were used to calibrate parameters, while the data collected on July 22 were used for performance evaluation. The test period was from 8:00 AM to 10:00 AM each day. This time period was chosen for two reasons: first, unexpected detection noises and errors caused by the video-based detectors could be avoided; second, the traffic condition did not change significantly and the signal timing plan did not change during this period.

## Parameter calibration

Based on Equation (10) and the feasible solution space [1.0, 5.0], two calibration strategies were tested in this study. One used the data from individual days; the other used the data from the entire three days. In addition to $\bar{h}$ and $\bar{h}_s$, several other parameters were used in the models and are summarized in Table 1. The calibration results are shown in Table 2.

As the calibration results show, $\bar{h}$ was larger than $\bar{h}_s$ when calibrated both by individual days and the entire three days. However, the parameter values varied when calibration was conducted by individual days. There are two potential reasons for this: one is the impact of detection errors; and the other is inadequate sample

**Table 2.** Parameter calibration results.

| Model | Period | Variable | Value | MSE | Total cycles | Cycles with QOD |
|---|---|---|---|---|---|---|
| Upstream-based input-output model | July 14, Tue. | $\bar{h}$ | 2.1 | 12992 | 70 | 27 |
| | | $\bar{h}_s$ | 1.9 | | | |
| | July 15, Wed. | $\bar{h}$ | 2.4 | 9332 | 71 | 32 |
| | | $\bar{h}_s$ | 1.6 | | | |
| | July 16, Thu. | $\bar{h}$ | 2.6 | 6372 | 71 | 30 |
| | | $\bar{h}_s$ | 2.1 | | | |
| | July 14–16 | $\bar{h}$ | 2.3 | 10042 | 211 | 89 |
| | | $\bar{h}_s$ | 1.8 | | | |
| Local-based input-output model | July 14, Tue. | $\bar{h}$ | 1.5 | 4704 | 70 | 27 |
| | July 15, Wed. | $\bar{h}$ | 1.7 | 1001 | 71 | 32 |
| | July 16, Thu. | $\bar{h}$ | 2.0 | 635 | 71 | 30 |
| | July 14–16[t] | $\bar{h}$ | 1.5 | 2238 | 211 | 89 |

size (number of cycles). Detection errors from the video detectors were the result of sensitivity to environmental factors, which could include light condition and vehicle color. More stable and consistent results could be expected from loop detector data. Therefore, the calibration results based on all three days were considered more reliable.

### *Performance evaluation*

Once calibrated, the proposed method was implemented using the data from 8:00 AM to 10:00 AM on July 22. The mean absolute error (MAE) and mean absolute percentage error (MAPE) were used as performance indexes, calculated by Equations (11) and (12). MAPE was calculated only for cycles with QOD because cycles with short queue lengths tended to generate meaninglessly large MAPE values even though the errors only represented a few vehicles.

$$MAE = \frac{1}{n}\sum_{i=1}^{n}\left|Q_i - \hat{Q}_i\right| \tag{11}$$

$$MAPE = \frac{1}{n}\sum_{i=1}^{n}\frac{Q_i - \hat{Q}_i}{Q_i} \tag{12}$$

Where $n$ is the total number of cycles, $Q_i$ is the ground truth maximum queue length, and $\hat{Q}_i$ is the estimated maximum queue length of the *ith* cycle. Recall that the proposed method includes three models. Only one model was used per cycle, depending on the QOD and misidentification checking process results. To illustrate the performance of the proposed method, a performance comparison between the proposed method and the individual models used independently was conducted, with results shown in Figure 8.

As shown in Figure 8, the proposed method showed significant improvements over the individual models, with a MAE of 35.7 ft. (approximately 1.4 vehicles) compared to 105.6 ft. (approximately 4.2 vehicles) using the breakpoint-based model and 61.8 ft. (approximately 2.5 vehicles) using the upstream-based input-output model. The breakpoint-based model had significant misidentification errors in multiple cycles (see cycles 8, 31, 33, 34, and 52 in Figure 8 (a) and (b)). Compared to the breakpoint-based model, the upstream-based input-output model tended to generate better results that were free of breakpoint misidentification issues; see Figure 6 (b) and (c). The local-based input-output model suitably estimated short queue lengths, while the breakpoint-based model could only estimate long queue lengths (see Figure 8 (b)), and the upstream-based model was occasionally affected by detection errors at the upstream intersection (see cycles 17–21 in Figure 8 (c)). It is also important to note that the MAPE was sensitive to occasional

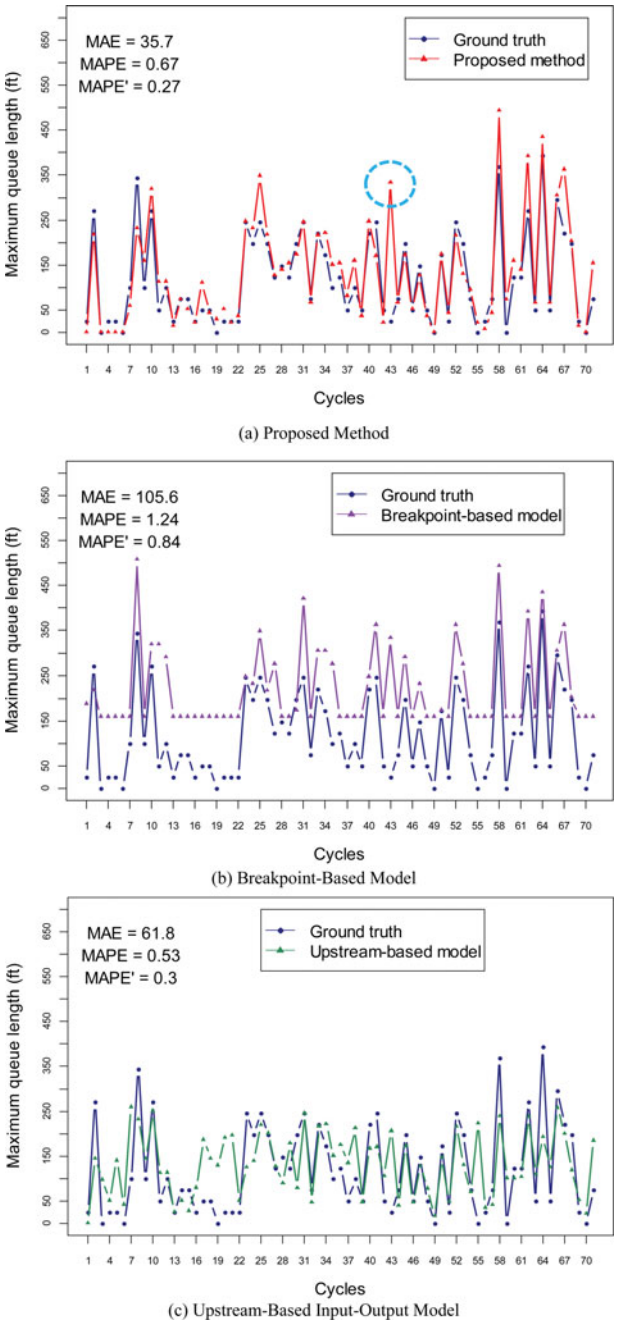


**Figure 8.** Estimated maximum queue length.

large estimation errors. This may be related to the relatively small sample size in this study. Based on the video of Cycle 31, the eastbound platoon released from Speedway at Mountain moved at an unusually slow progression speed and did not join the end of the queue at Speedway and Park, causing the proposed method to overestimate the queue length. However, by removing this outlier (circled in blue in Figure 8(a)), the MAPEs of all three models dropped dramatically as indicated by the MAPE' values shown in Figure 8. The situation observed in Cycle 31 was rarely observed in other cycles.

**Table 3.** Model performance measures based on cycle type.

| Cycle Scenario | MAEs (ft.) | | |
|---|---|---|---|
| | Local-based input-output model | Upstream-based input-output model | Breakpoint-based model |
| 1 | 59.2 | 102.7 | — |
| 2 | — | 38.7 | 143.5 |
| 3 | — | 77.0 | 66.9 |

To further illustrate the effectiveness of the proposed method, each of the three models was evaluated separately with groups of cycles with different traffic conditions. Based on cycle type, three scenarios were defined: cycles without QOD (Scenario 1), cycles with QOD and misidentification (Scenario 2), and cycles with QOD and without misidentification (Scenario 3). The resultant MAEs are summarized in Table 3.

As shown in Table 3, the MAEs in Scenario 1 indicated that the local-based model was more suitable to estimate short queue lengths than the upstream-based model. In Scenario 2, the large MAE of the breakpoint-based model (almost four times larger than that of the upstream-based model) indicated that the misidentification of point C did occur, and the upstream-based model was more reliable. For Scenario 3, the breakpoint-based model was more accurate compared to the upstream-based model.

Although significant improvement in maximum queue length estimates were achieved using the proposed method compared to the breakpoint-based model, several limitations and concerns are also discussed here. In this study, two parameters, $\bar{h}$ and $\bar{h}_s$, were defined in the input-output models. These parameters are crucial to the accuracy of maximum queue length estimation in situations where the breakpoint-based model is not reliable. Model calibration was based on ground truth queue lengths at the test site during a time period with various traffic conditions. Based on the assumptions of the proposed model and the nature of urban traffic flow, two potential issues may arise in extensional applications. One is whether the calibrated parameters could be used for time periods other than those associated with calibration. The other issue is whether each intersection needs an exclusive calibration process. Each issue is elaborated as follows.

(1) *Validity of the parameters for different time periods*. When applied to a much longer time period (e.g., 24 hours), the parameters calibrated in a typical period may not be reliable, especially for the upstream-based model. Reliability could be expected if correlation (e.g., in proportion) between the upstream input flow and the downstream maximum queue length is well sustained during different time periods. Therefore, obtaining desirable parameters for different traffic patterns may require considerable effort.

(2) *Transferability of parameters among intersections*. Although exclusive calibrations are desirable to enhance the local performance of the proposed model, it is almost impossible in a large road network since collection of ground truth queue length is time-consuming and costly. The parameters for one typical intersection may be transferable to other similar intersections. However, such "similarity" could depend on many factors, such as speed limits, mid-block disturbance, driver behavior, detector locations, and detector type.

## Conclusion

This paper proposed a real-time maximum queue length estimation method using high-resolution event-based data specifically with single-channel detection. A misidentification checking process and two input-output models (upstream-based and local-based) based on a simple input flow rate estimation model were proposed to address the overestimation and short queue length estimation problems of the breakpoint-based model. The misidentification checking process and input-output models were integrated with the breakpoint-based model and a QOD identification process to create an effective framework for measuring real-time queue length. The proposed method was implemented and evaluated using field-collected event-based data from Speedway Boulevard in Tucson, Arizona.

Important conclusions from this paper include: (1) significant queue estimation improvements were achieved using the proposed method, with a maximum queue length estimation MAE of 35.7 ft. compared to 105.6 ft. using solely the breakpoint-based model; (2) the local-based input-output model can estimate short queue lengths with satisfactory accuracy; (3) the misidentification checking process and upstream-based input-output model were effective in addressing the overestimation of the breakpoint-based model.

In the future, it is recommended to collect more data for investigating validity and transferability of model parameters. Also, the effectiveness of the proposed model could be further verified using other types of detectors (e.g., loop detectors).

## Acknowledgments

The authors would like to thank the City of Tucson for their data support. We would also like to thank Michael Hicks, Bob Hunt, Paul Casertano, Simon Ramos, Jorge Riveros, and Francisco Leyva for providing valuable advice and technical

support in this project. Special thanks go to Payton Cooke for his proofreading assistance.

## Funding

We are grateful to China Xinjiang Autonomous Region Science and Technology Support Project (No. 201332112) for funding support.

## References

Anusha, S. P., Sharma, A., Vanajakshi, L., Subramanian, S. C., & Rilett, L. R. (2016). Model-based approach for queue and delay estimation at signalized intersections with erroneous automated data. *Journal of Transportation Engineering*, *142*(5), 04016013.

Ban, X. J., Hao, P., & Sun, Z. (2011). Real time queue length estimation for signalized intersections using travel times from mobile sensors. *Transportation Research Part C: Emerging Technologies*, *19*(6), 1133–1156.

Cheng, Y., Qin, X., Jin, J., Ran, B., & Anderson, J. (2011). Cycle-by-cycle queue length estimation for signalized intersections using sampled trajectory data. *Transportation Research Record: Journal of the Transportation Research Board*, (2257), 87–94.

Cheng, Y., Qin, X., Jin, J., & Ran, B. (2012). An exploratory shockwave approach to estimating queue length using probe trajectories. *Journal of Intelligent Transportation Systems*, *16*(1), 12–23.

Chang, J., Talas, M., & Muthuswamy, S. (2013). Simple methodology for estimating queue lengths at signalized intersections using detector data. *Transportation Research Record: Journal of the Transportation Research Board*, (2355), 31–38.

Comert, G., & Cetin, M. (2009). Queue length estimation from probe vehicle location and the impacts of sample size. *European Journal of Operational Research*, *197*(1), 196–202.

Claudel, C., Hofleitner, A., Mignerey, N., & Bayen, A. (2009). *Guaranteed bounds on highway travel times using probe and fixed data*. 88th TRB Annual Meeting Compendium of Papers.

Day, C. M., Bullock, D. M., Li, H., Remias, S. M., Hainen, A. M., Freije, R. S., & Brennan, T. M. (2014). Performance measures for traffic signal systems: an outcome-oriented approach. Technical Report, Purdue University, Lafayette, IN. http://dx.doi.org/10.5703/1288284315333

Geroliminis, N., & Skabardonis, A. (2005). Prediction of arrival profiles and queue lengths along signalized arterials by using a Markov decision process. *Transportation Research Record: Journal of the Transportation Research Board*, (1934), 116–124.

Geroliminis, N., & Skabardonis, A. (2006). *Real time vehicle reidentification and performance measures on signalized arterials*. 2006 IEEE Intelligent Transportation Systems Conference (pp. 188–193). IEEE.

Hu, H., Wu, X., & Liu, H. X. (2013). Managing oversaturated signalized arterials: a maximum flow based approach. *Transportation Research Part C: Emerging Technologies*, *36*, 196–211.

Hao, P., Ban, X. J., Guo, D., & Ji, Q. (2014). Cycle-by-cycle intersection queue length distribution estimation using sample travel times. *Transportation research part B: methodological*, *68*, 185–204.

Hao, P., Ban, X., & Whon Yu, J. (2015). Kinematic equation-based vehicle queue location estimation method for signalized intersections using mobile sensor data. *Journal of Intelligent Transportation Systems*, *19*(3), 256–272.

Hao, P., & Ban, X. (2015). Long queue estimation for signalized intersections using mobile data. *Transportation Research Part B: Methodological*, *82*, 54–73.

Highway Capacity Manual. (2010). Transportation Research Board of the National Academies. Washington, D.C.

Liu, H. X., Wu, X., Ma, W., & Hu, H. (2009). Real-time queue length estimation for congested signalized intersections. *Transportation Research Part C: Emerging Technologies*, *17*(4), 412–427.

Liu, H. X., & Ma, W. (2009). A virtual vehicle probe model for time-dependent travel time estimation on signalized arterials. *Transportation Research Part C: Emerging Technologies*, *17*(1), 11–26.

Lieberman, E., Chang, J., & Prassas, E. (2000). Formulation of real-time control policy for oversaturated arterials. *Transportation Research Record: Journal of the Transportation Research Board*, (1727), 77–88.

Lieberman, E., & Chang, J. (2005). Optimizing traffic signal timing through network decomposition. *Transportation Research Record: Journal of the Transportation Research Board*, (1925), 167–175.

Lighthill, M. J., & Whitham, G. B. (1955). *On kinematic waves. I. Flood movement in long rivers. Proceedings of the Royal Society of London A: Mathematical, Physical and Engineering Sciences*, *229*(1178), 281–316.

Lee, S., Wong, S. C., & Li, Y. C. (2015). Real-time estimation of lane-based queue lengths at isolated signalized junctions. *Transportation Research Part C: Emerging Technologies*, *56*, 1–17.

Michalopoulos, P. G., Stephanopoulos, G., & Pisharody, V. B. (1980). Modeling of traffic flow at signalized links. *Transportation Science*, *14*(1), 9–41.

Mück, J. (2002). Using detectors near the stop-line to estimate traffic flows. *Traffic engineering & control*, *43*(11), 429–434.

Mück, J. (2009). *The german network control method motion—new methods and evaluations*. 16th ITS World Congress and Exhibition on Intelligent Transport Systems and Services.

Newell, G. F. (1960). Queues for a fixed-cycle traffic light. *The Annals of Mathematical Statistics*, *31*(3), 589–597.

Richards, P. I. (1956). Shock waves on the highway. *Operations research*, *4*(1), 42–51.

Robertson, D. I. (1969). *TRANSYT: A traffic network study tool* (Road Research Laboratory Report LR 253). Crowthorne, United Kingdom: Road Research Laboratory.

Robertson, D. I., & Bretherton, R. D. (1991). Optimizing networks of traffic signals in real time: The SCOOT method. *IEEE Transactions on Vehicular Technology*, *40*(1), 11–15.

Sharma, A., Bullock, D., & Bonneson, J. (2007). Input-output and hybrid techniques for real-time prediction of delay and maximum queue length at signalized intersections. *Transportation Research Record: Journal of the Transportation Research Board*, (2035), 69–80.

Stephanopoulos, G., Michalopoulos, P. G., & Stephanopoulos, G. (1979). Modelling and analysis of traffic queue dynamics

at signalized intersections. *Transportation Research Part A: General*, *13*(5), 295–307.

Strong, D. W., & Rouphail, N. M. (2006). *Incorporating effects of traffic signal progression into proposed incremental queue accumulation method*. Transportation Research Board 85th Annual Meeting (No. 06–0107).

Skabardonis, A., & Geroliminis, N. (2008). Real-time monitoring and control on signalized arterials. *Journal of Intelligent Transportation Systems*, *12*(2), 64–74.

Tian, Z., & Urbanik, T. (2006). Green extension and traffic detection schemes at signalized intersections. *Transportation Research Record: Journal of the Transportation Research Board*, (1978), 16–24.

Viti, F., & van Zuylen, H. (2004). Modeling queues at signalized intersections. *Transportation Research Record: Journal of the Transportation Research Board*, (1883), 68–77.

Viti, F., & Van Zuylen, H. J. (2009). The dynamics and the uncertainty of queues at fixed and actuated controls: A probabilistic approach. *Journal of Intelligent Transportation Systems*, *13*(1), 39–51.

Webster, F. V. (1958). Traffic signal settings. *Road research technical paper 39*. London, England: Road Research Laboratory, Her Majesty's Stationery Office.

Wu, Y. J., Zhang, G., & Wang, Y. (2010). Volume data correction for single-channel advance loop detectors at signalized intersections. *Transportation Research Record: Journal of the Transportation Research Board*, (2160), 128–139.

Wu, Y. J., An, S., Ma, X., & Wang, Y. (2011). Development of web-based analysis system for real-time decision support on arterial networks. *Transportation Research Record: Journal of the Transportation Research Board*, (2215), 24–36.

Zheng, J., Ma, X., Wu, Y. J., & Wang, Y. (2013). Measuring signalized intersection performance in real-time with traffic sensors. *Journal of Intelligent Transportation Systems*, *17*(4), 304–316.